First-Principles Calculations of Structural, Electronic, Optical, and Thermoelectric Properties of LuNiBi and LuNiSb Half-Heusler

Amina Touia[1] · Karima Benyahia[1] · Adem Tekin[2]

Abstract

The structural, electronic, optical, and thermo-electric properties of LuNiBi and LuNiSb Half-Heusler have been studied using a full potential linearized augmented plane-wave (FP-LAPW) method. The results of the calculations presented in this work were obtained through the use of different approximations GGA-PBE, GGA-PBEsol, GGA-WC, and mBJ-GGA. The electronic band structures exhibit that the LuNiBi and LuNiSb alloys have a small indirect gaps in the valence band and the conduction band at points Γ and X, revealing the semiconductor character in both compounds. The complex dielectric function $\varepsilon(\omega)$, optical conductivity $\sigma(\omega)$, extinction coefficient $\kappa(\omega)$, refractive index $n(\omega)$, and reflectivity $R(\omega)$ as a function of photon energy are calculated using mBJ-GGA approximation, that is yielding results in good accordance with available experimental data. On the other hand, the variations of the thermal conductivity, power factor, figure of merit ZT, Seebeck coefficient, and electrical conductivity, as a function of temperature, have been investigated. Most of the optical and thermoelectric properties of LuNiSb and LuNiBi materials are not available in the literature; this makes the present work as a detailed comparative study between both compounds and opens the path for other future accurate theoretical studies to find the promising substitute for the interesting and more efficient thermoelectric device in industry.

Keywords LuNiBi · LuNiSb · FP-LAPW · GGA-PBEsol · GGA-WC · Semiconductor · Extinction coefficient $\kappa(\omega)$ · Thermal conductivity · Refractive index $n(\omega)$

1 Introduction

The present work is an ab initio study of the physical properties (structural, electronic, optical, and thermo-electric) of LuNiBi and LuNiSb alloys based just on bismuth and antimony using the FP-LAPW method (full-potential linearized augmented plane wave) method implemented in the WIEN2K code [1], which has demonstrated the extraordinary efficiency and which gives the general ideas on all digital tools. Materials based on bismuth and antimony have been intensively studied because of their many technological applications, especially in the field of optoelectronics and thermo-electric [2, 3, 6]. Half-Heusler, a type of alloy, is chemically defined by the formula XYZ [4, 5]. It crystallizes in a cubic structure (shown in Fig. 1) of space group F-43 m C1b (group no. 216), where the elements X, Y, and Z, respectively, occupy the Wyckoff positions 4a, 4b, and 4c in the phase most ordered chemical [2, 3, 6, 7]. The electronic band structures exhibit that the LuNiBi and LuNiSb alloys have a small indirect gaps in the valence band and the conduction band at points Γ and X. This means that the LuNiBi and LuNiSb are semiconductors. The theoretical results obtained for band structures are in good agreement with those found experimentally [2, 6]. We have studied optical and thermo-electric parameters as a function of photon energy and as a function of temperature respectively using mBJ-GGA approximation in which we have had good results.

2 Computational Method

This research is designed to study the physical properties of Half-Heusler LuNiBi and LuNiSb compounds. DFT calculations [8] were performed using the full-potential
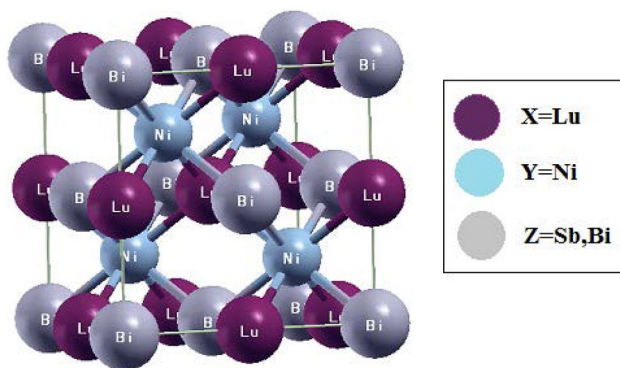
✉ Amina Touia
  anima11@live.fr

1 Materials Science and Applications Laboratory, Faculty of Sciences and Technology, University of Ain Temouchent, Belhadj Bouchaib. BP 284, 46000 Ain-Temouchent, Algeria

2 Informatics Institute, Istanbul Technical University, 34469 Maslak, Istanbul, Turkey

Fig. 1 Crystal structure of LuNiZ (Z = Sb, Bi)

linearized augmented plane wave (FP-LAPW) method implemented in the WIEN2K code [1], and to determine the potential for exchange and correlation, several approximations used GGA (PBE96, WC, and PBEsol) [9–11] and the approximation of modified Becke-Johnson (mBJ) [8]. The energy cut-off parameter between the core and valence state was chosen equal to -6.0 Ry. We have chosen the Muffin-Tin radii (RMT) equal to Lu = 2.45, Ni = 2.45, and Bi = 2.30 (atomic unit) for LuNiBi and Lu = 2.5, Ni = 2.5, and Sb = 2.35 (u.a) for LuNiSb, respectively. The reciprocal space has been sampled with k-points grid (5000 k-points) in the first brillouin zone (BZ) that corresponds to 150 K-points in irreducible BZ. The plane waves are limited to $RMT \times Kmax = 9$.

3 Results and Discussion

3.1 Structural Properties

In the first step, we carried out a systematic theoretical study of structural properties (lattice parameter, bulk modulus, and its derivatives). Figure 2 shows the total energy versus volume curves for the two materials LuNiBi and LuNiSb, respectively. The calculations were performed using the three approximations of the exchange and correlation potential, GGA-PBE, GGA-WC, and GGAPBEsol. Fitting of these curves using the Birch Murnaghan equation of state [12] yields values of a_0, B_0, and B'_0 in good agreement with the experimental results [2, 3, 6] as it is displayed in Table 1. Therefore, the values obtained for the lattice parameters are overestimated compared to the experimental results due to the use of GGA-(PBE, WC, PBEsol). The lattice parameter, bulk modulus, and its pressure derivatives obtained for LuNiBi and LuNiSb are in good agreement with the available experimental and theoretical data [13–15]. We also note that the GGA-PBE approximation always has the lowest total energy unlike the other approximations (PBEsol and WC) for the two materials LuNiBi and LuNiSb. This means that the structure is more stable for the GGA-PBE approximation.

3.2 Electronic Properties

The electron energy band structures of LuNiBi and LuNiSb were calculated along high lines of symmetry in
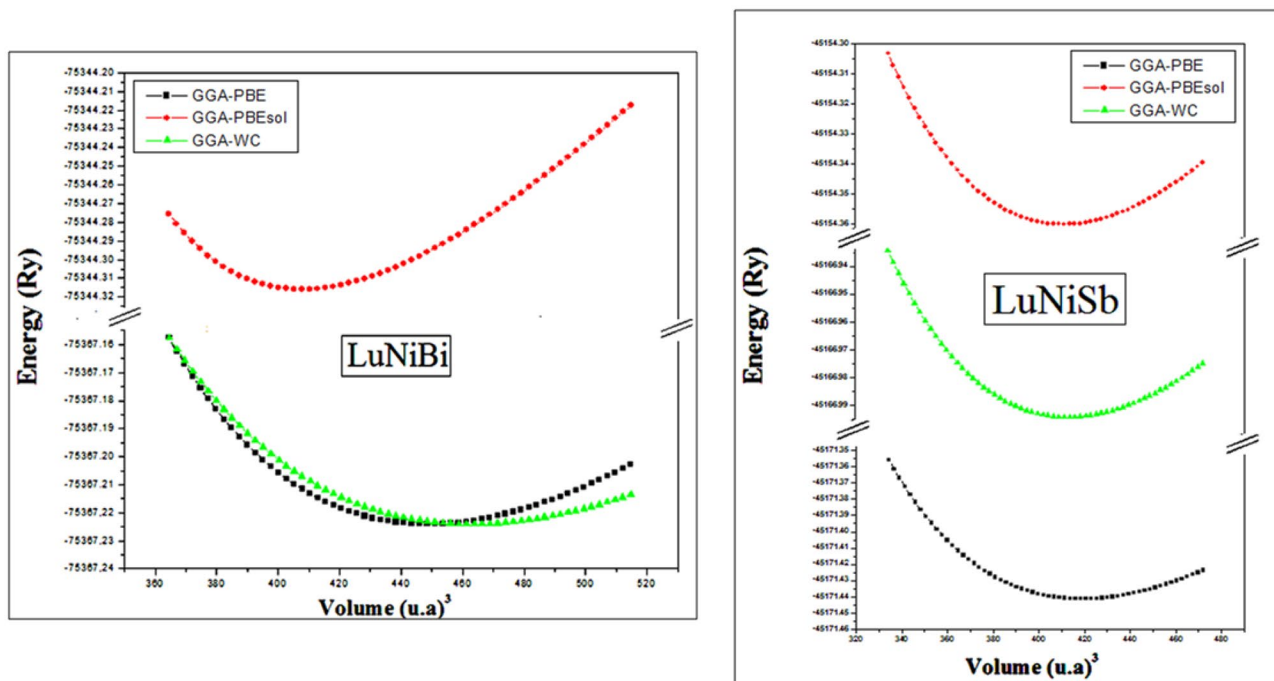
Fig. 2 Total energy versus volume curves of LuNiZ (Z = Bi, Sb) using GGA (PBE96, PBEsol, and WC)

Table 1 Lattice constant a_0 (in Å), bulk modulus B (in GPa), its pressure derivative B', and minimum energy at equilibrium E_0 (in Ryd) using GGA (PBE96, PBEsol, and WC)

Present work	a_0 (Å)	B (GPa)	B'	E_0 (Ry)
LuNiBi				
GGA-PBE	6.4309	82.6840	4.5964	−75,367.224079
GGA-PBEsol	6.3228	95.0379	5.1427	−75,344.315982
GGA-WC	6.4306	82.6293	4.6195	−75,367.224055
Experimental	6.335 [6–13]	-	-	-
Other calc	6.4180 [14]	81.752 [14]	4.642 [14]	-
	6.2387 [14]	102.915 [14]	4.718 [14]	-
LuNiSb				
GGA-PBE	6.2866	95.7671	4.4107	−45,171.441390
GGA-PBEsol	6.1903	110.8236	4.4132	−45,154.360274
GGA-WC	6.1988	110.1933	4.3594	−45,166.994128
Experimental	6.155 [2]	-	-	-
Other calc	6.277 [15]	112.95 [15]		

the Brillouin zone [16]. The results obtained are calculated across different potentials using the GGA approximation. The usual problem of underestimating the DFT gap has encouraged researchers to find an appropriate solution; mBJ is a modified version of the exchange potential proposed by modified Becke-Johnson (mBJ) [9]. This mBJ-GGA version was also used in order to find the forbidden band in better agreement with the experimental band gap. The results obtained are shown schematically in Fig. 3 for LuNiBi and LuNiSb, respectively. The two compounds have small indirect gaps following the Γ-X direction, where the valence band maximum is located at point Γ and the conduction band minimum is at point X. Consequently, the two materials studied present a semiconductor character. In Table 2,

we display together the different gap values of the two compounds, for the two approximations GGA-PBE and GGA-mBJ. Good agreement between the theoretical and experimental results is confirmed [13–17]. The electronic density of states is one of the most interesting electronic properties in solid state physics. We calculated the total (TDOS) and partial (PDOS) density of state in each compound using the mBJ-GGA. The results obtained are illustrated in Figs. 4 and 5. The energy of the Fermi level (E_F) is indicated by a dashed vertical line located at 0.0 eV ($E_F = 0.0$ eV). The main characteristics occur between the energy interval of the Fermi level $E_F - 15.0$ eV and $E_F + 10.0$ eV for the two compounds. The valence band of each compound is mainly dominated by the states of the Lu-f and Ni-d orbitals, with

Fig. 3 The band structure of LuNiZ ($Z = $ Bi, Sb) at the equilibrium structure using mBJ-GGA approximation
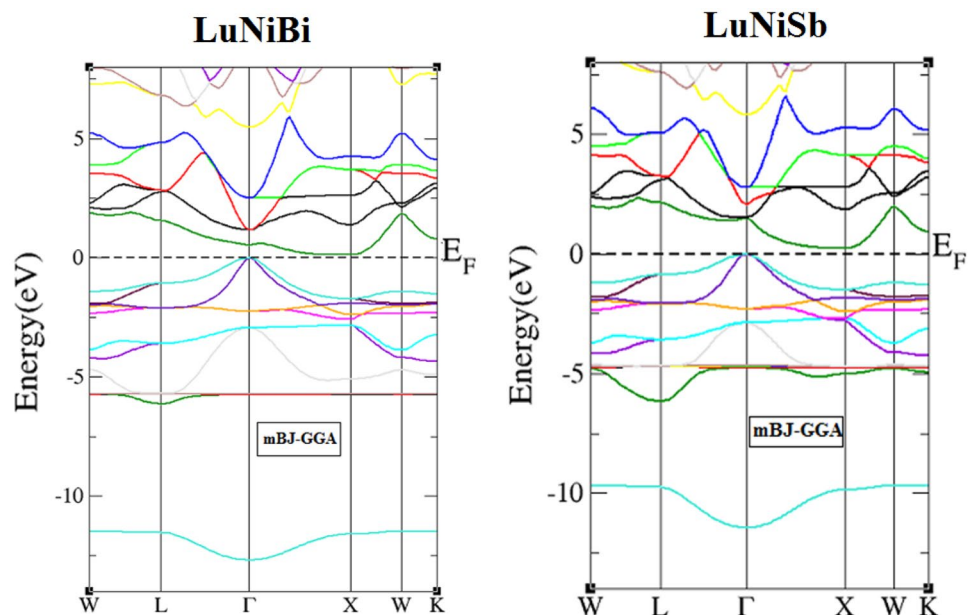
Table 2 The calculated values of band gap of LuNiZ (Z = Bi, Sb) at $T = 0$ K and $P = 0$ GPa

Present work	Indirect gap (eV) Γ -X
	LuNiBi
mBJ-GGA	0.12
GGA-PBE	0.113
Experimental	0.116 [6]
	0.121 [3]
Other calc	0.20 [13]
	LuNiSb
mBJ-GGA	0.220
GGA-PBE	0.148
Experimental	0.190 [2]
Other calc	0.200 [15]
	0.078 [16]
	0.227 [17]

small contribution from the Bi-s, Bi-p, Sb-s, and Sb-p orbitals for LuNiBi and LuNiSb, respectively. The conduction band is mainly formed by the states of the orbitals Lu-d, Ni-d, Bi-p, and Sb-p, for LuNiBi and LuNiSb, respectively.

3.3 Optical Properties

In the calculations of the optical properties of the compounds LuNiBi and LuNiSb, we used the GGA-mBJ (modified Becke-Johnson) [9]. The results of calculations of the imaginary part ε_2 (ω) and of the real (dispersive) part ε_1 (ω) of the dielectric function [18–20] in the energy range from 0 to 13.5 eV for these compounds are illustrated in Fig. 6a–b. Analysis of these spectra shows that the first critical points of the imaginary part ε_2 (ω) of the dielectric function which corresponds to the fundamental absorption thresholds starts at around 0.11 eV and 0.22 eV for LuNiBi and LuNiSb, respectively. The origin of these points is due to the optical transition between the highest valence band and the lowest conduction band, and then, the values of the critical points correspond to the transition (Γv-Xc) for LuNiBi and LuNiSb. Thus, we notice next to the fundamental peak the main peaks, which reflect the maximum absorption, are located at 2.1 eV for the two compounds. The calculated results of the real part ε_1 (ω) show that the zero crossing of the two spectra means the non-existence of scattering. We have noticed that for all these compounds, the function ε_1 (ω) is canceled at the following energy values: 4.7 eV (LuNiBi) and 5.7 eV (LuNiSb), where the dispersion at these energy values is zero, and therefore, the absorption is maximum. The reflectivity spectra R (ω) [21–23] of the compounds LuNiBi and LuNiSb are illustrated in Fig. 7a.

The evolution of these spectra shows that the values of the reflectivity R (ω) of the two compounds reach a maximum value at peaks 65% and 68%, respectively. The refractive index n (ω) spectra [21–23] of the compounds LuNiBi and LuNiSb are shown in Fig. 7b. The evolution of these spectra shows that the values of the refractive index n (ω) of the two compounds reach a maximum value at energies 1.31 eV and 1.25 eV, respectively.

The extinction coefficient κ (ω) [21–23] of the compounds LuNiBi and LuNiSb are shown in Fig. 8a. Their evolution shows that the values of the extinction coefficient κ (ω) of the two compounds reach a maximum value at energies 5.96 eV and 6.72 eV, respectively. If optical conductivity is synonymous with the presence of free charge in the conduction band, then in our case (semiconductor at $T = 0$ K), this means that electrons in the valence band have acquired sufficient energy to cross the gap. We can therefore estimate that the minimum energy threshold to have a conduction value is the point on the energy axis where the curve of σ (ω) takes a considerable ascending pace. This energy threshold is in fact only the indirect optical gap. A reading of Fig. 8b reveals the following optical gaps: LuNiBi: $E_g = 0.12$ eV and LuNiSb: $E_g = 0.22$ eV.

3.4 Thermoelectric Properties

-Thermoelectricity transforms heat into electricity. In this case, it is the heat flow that causes a displacement of the charge carriers and therefore the appearance of an electric current. At first, we examine the effect of temperature on electrical conductivity, Seebeck coefficient, thermal conductivity, power factor, and figure of merit [24, 25].

-The curves of electrical conductivity as a function of temperature are shown in Fig. 9a. The electrical conductivity of LuNiBi and LuNiSb compounds increases with temperature. It reaches a maximum value of 1.48×10^{19} (1/Ω cm s) and 1.1×10^{19} (1/Ω cm s) for a temperature of 1000 K, respectively.

Figure 9b shows the change in the Seebeck coefficient as a function of temperature. The positive sign of the Seebeck coefficient (S > 0) for the LuNiBi and LuNiSb suggests a conduction of the material made by holes; therefore, this material is of type p (S > 0). In these figures, we notice that the amplitude of the Seebeck coefficient S deprived with the increase of temperature at $T = 200$ K (LuNiBi) and $T = 350$ K (LuNiSb), respectively. Then, we calculate the seebeck coefficient and we notice that the electrical conductivity varies in opposite ways. The results found within this study agree well with experimental findings [7–17].
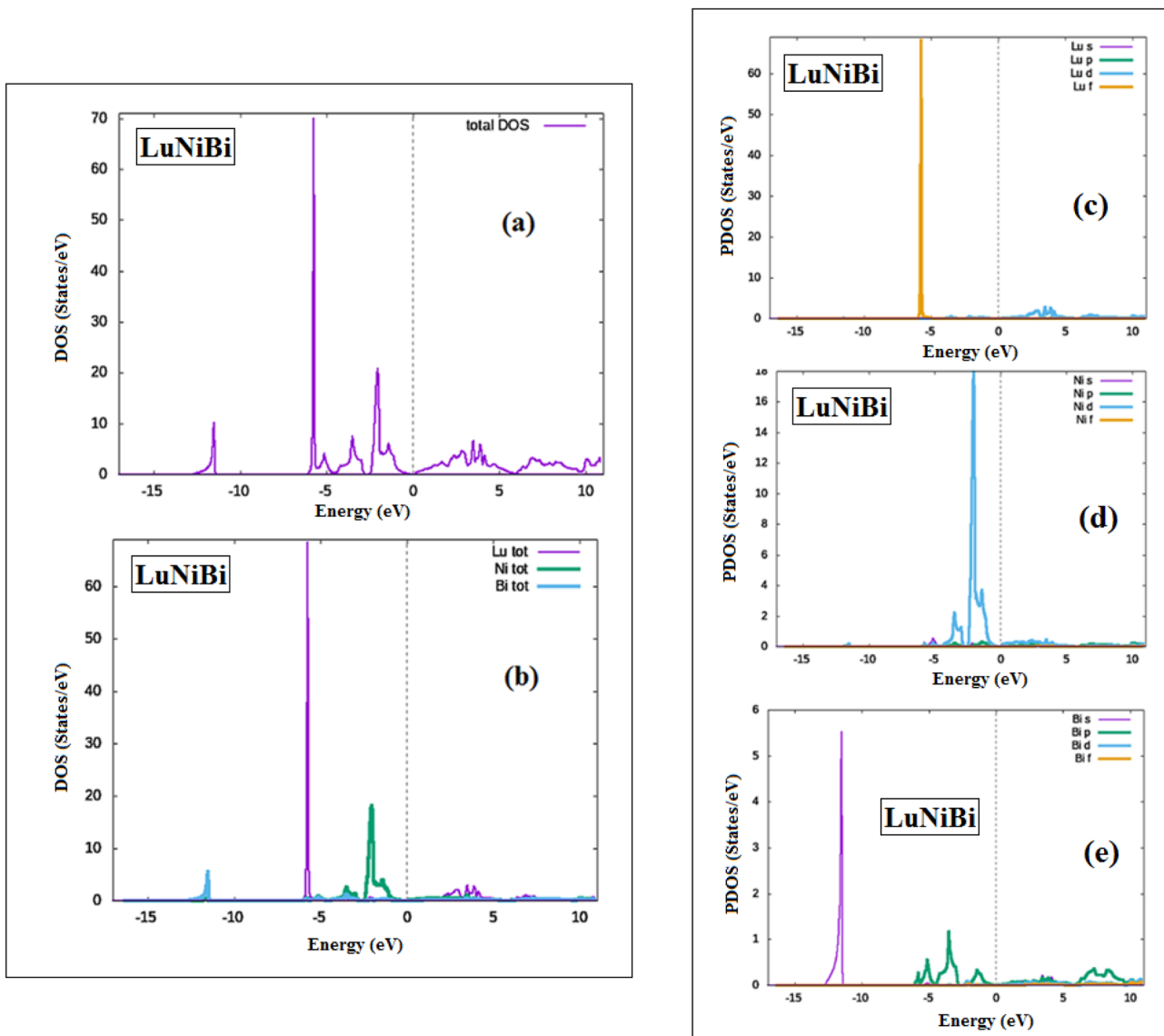
Fig. 4 The total (**a**, **b**) and partial density of states (**c**, **d**, **e**) of LuNiBi: at the equilibrium structure using mBJ-GGA approximation

-Thermal conductivity is composed of two terms, a term which depends on the lattice parameter and an electronic term, knowing that each term has different temperature dependence. At room temperature, thermal conductivity is mainly affected by the structure of the network (over 98%) [26]. Figure 9c shows a higher thermal conductivity of LuNiBi and LuNiSb which increases continuously with temperature.

-The variation in power factor as a function of temperature is presented in Fig. 10a. The LuNiBi has a distinct behavior; its power factor reaches a maximum value at 400 K, then decreases rapidly (an exponential drop) from this temperature, and becomes zero above 1000 K.

A similar behavior is observed for the LuNiSb material at temperature 700 K, but does not drop zero above 1000 K. The results found within this study agree well with theoretical findings [15, 16].

-The variation in figure of merit as a function of temperature is presented in Fig. 10b. The figure of merit curves are decreasing for these two materials LuNiBi and LuNiSb over the whole temperature range. The higher value of $ZT = 0.76$ (LuNiBi) and $ZT = 0.81$ (LuNiSb) is mainly due to its great thermal conductivity (the figure of merit is defined as $ZT = S^2 \sigma T / \kappa$) [27]. The results found within this study agree well with theoretical findings [17].
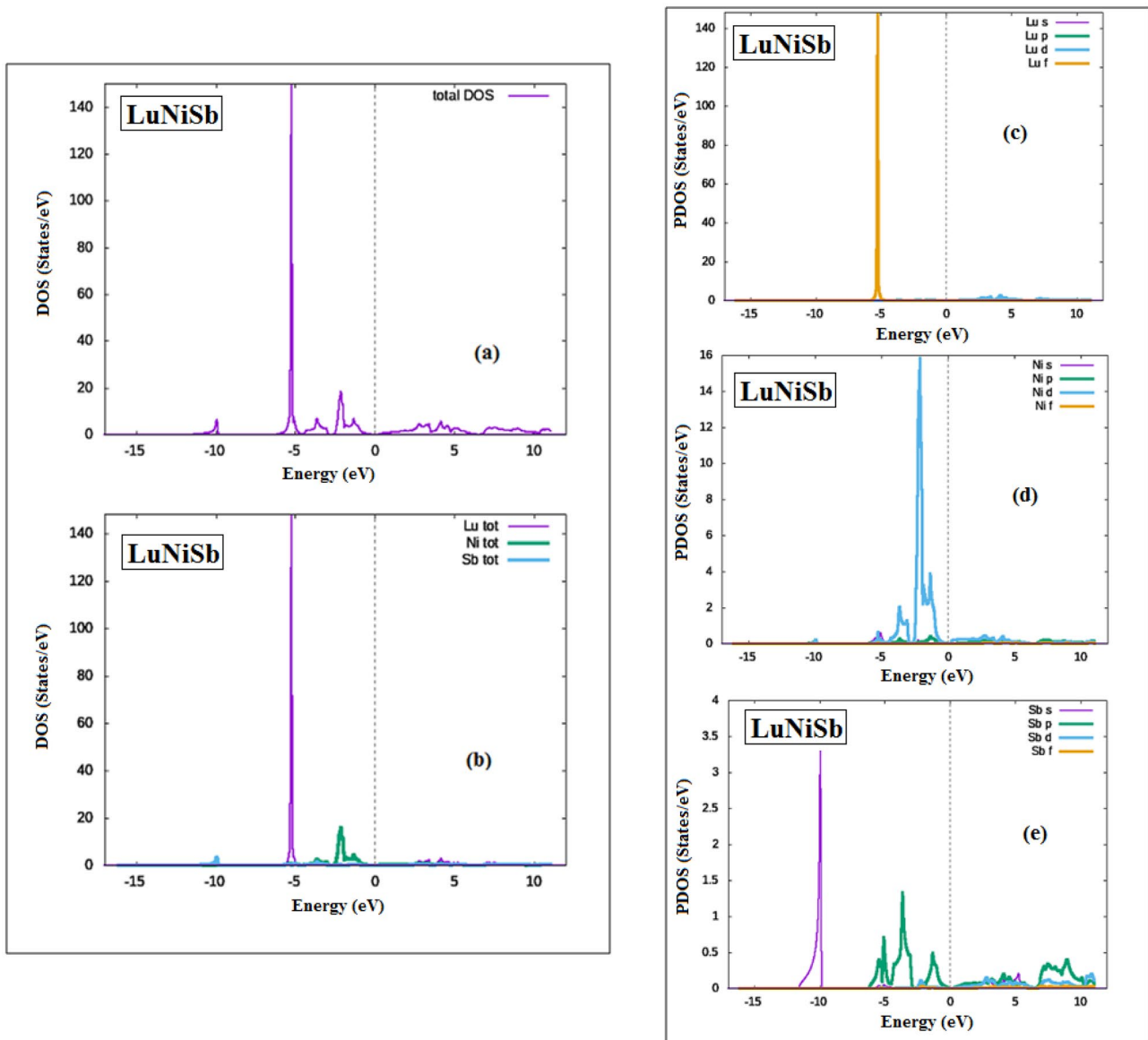
Fig. 5 The total (**a**, **b**) and partial density of states (**c**, **d**, **e**) of LuNiSb: at the equilibrium structure using mBJ-GGA approximation
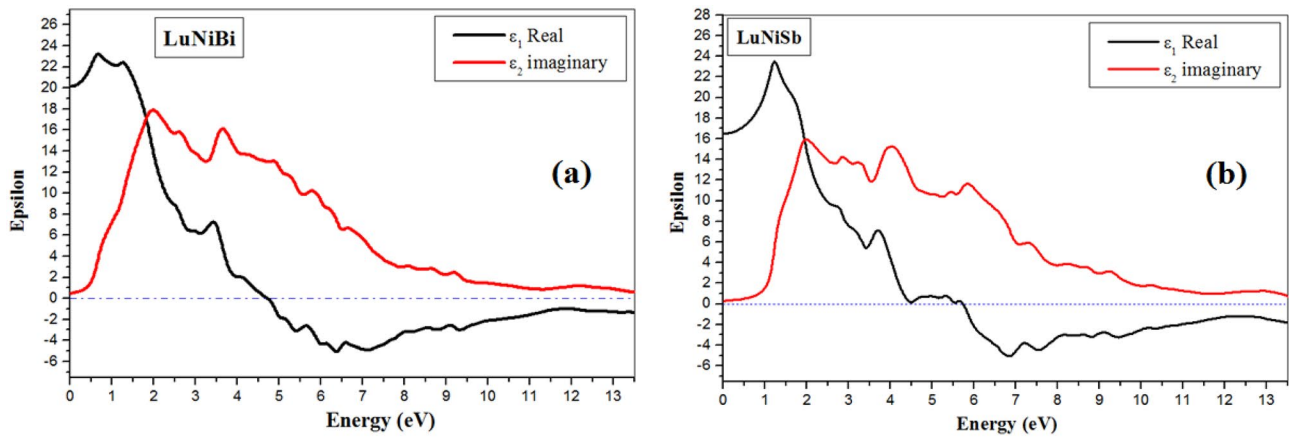
Fig. 6 Real part of dielectric function (ε_1 (ω)) and Imaginer part of dielectric function (ε_2 (ω)) of LuNiZ (Z=Bi, Sb) compounds (**a**, **b**)
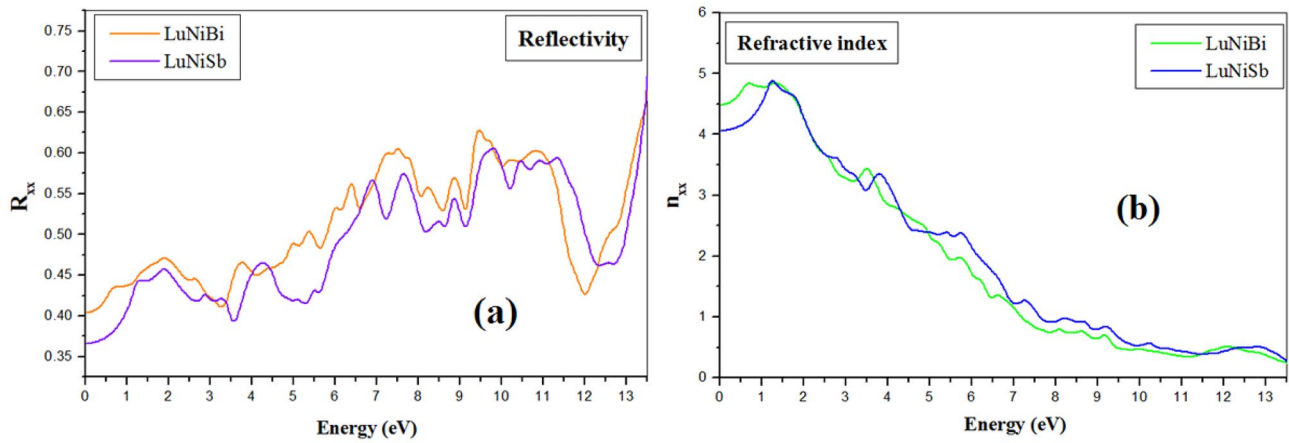

Fig. 7 The reflectivity (R (ω)) (**a**) and refractive index (n (ω)) (**b**) of LuNiZ (Z=Bi, Sb) compounds
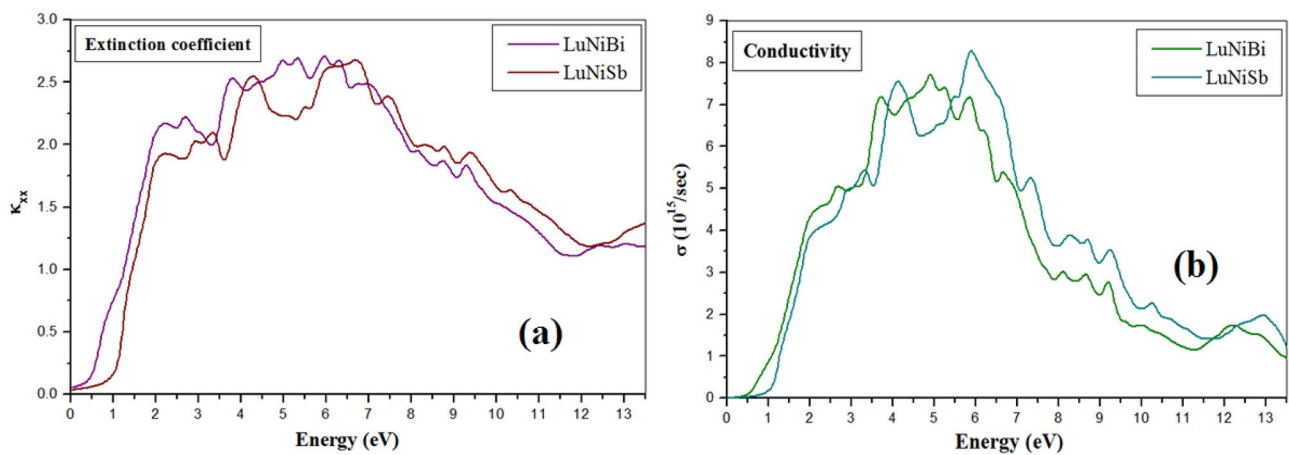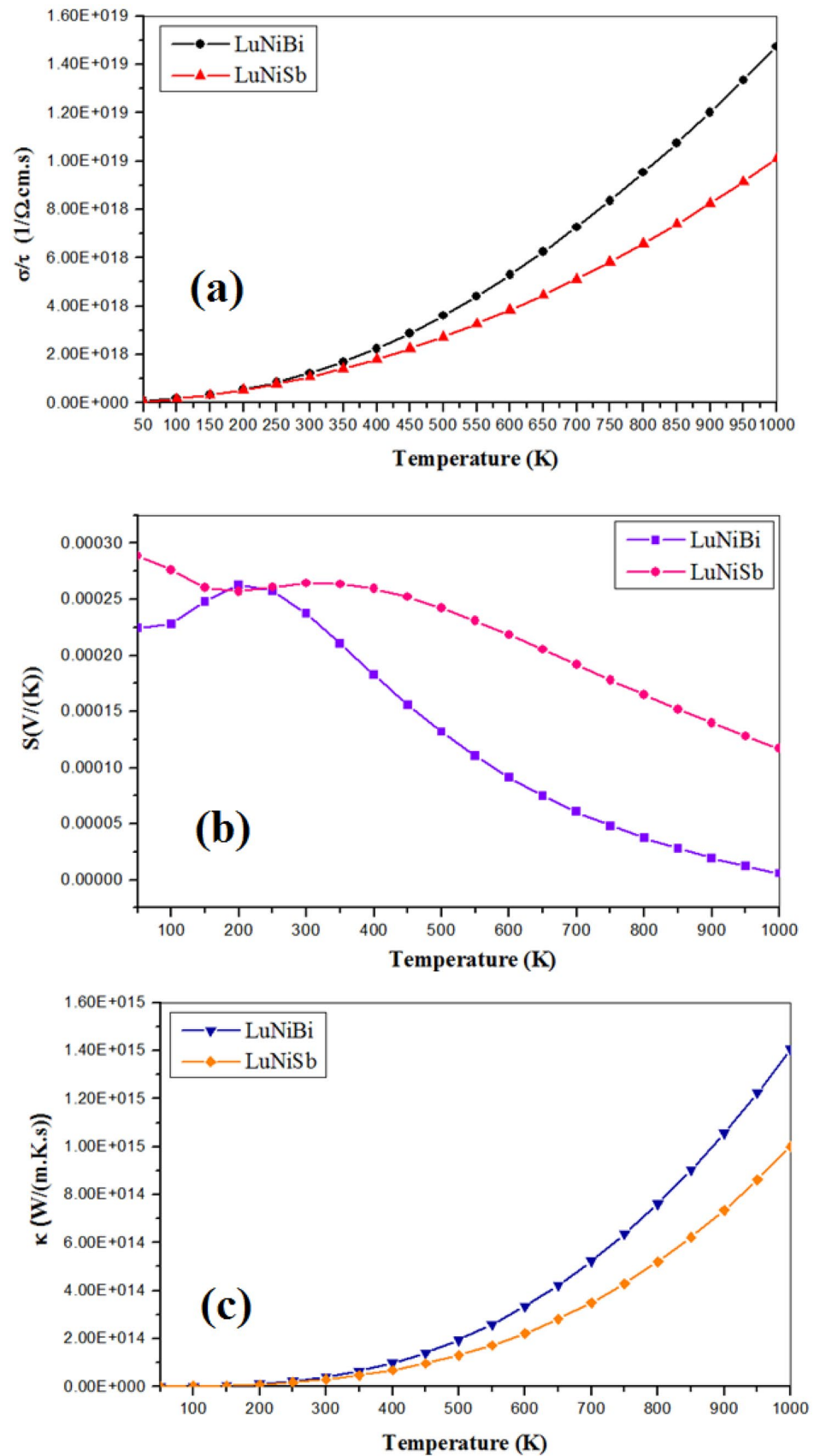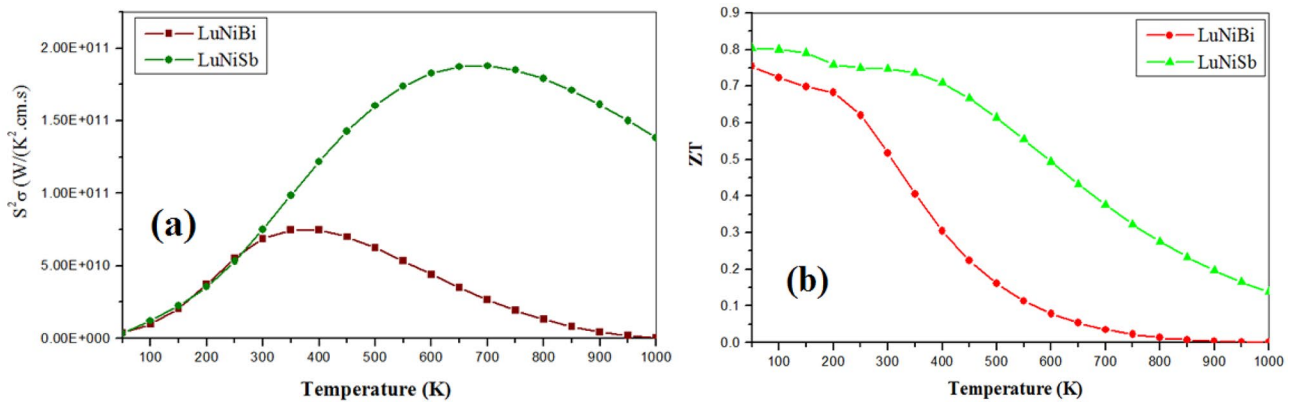

Fig. 8 The extinction coefficient (κ (ω)) (**a**) and conductivity σ (ω) (**b**) of LuNiZ (Z=Bi, Sb) compounds

Fig. 9 The variation of the electrical conductivity (**a**), Seebeck coefficient (**b**), and thermal conductivity (**c**), as a function of temperature for LuNiBi and LuNiSb

Fig. 10 The power factor (**a**) and figure of merit ZT (**b**) as a function of temperature for LuNiBi and LuNiSb

4 Conclusion

To sum up, a comparative study of the structural, electronic, optical, and thermo-electric properties of the two Half-Heusler materials based on bismuth (Bi) and antimony (Sb) has been investigated. The full potential linearized augmented plane-wave (FP-LAPW) has been used within density functional theory (DFT), and the potential for exchange and correlation is treated by different approximations: the generalized gradient approximation GGA (PBE96, WC, PBEsol) and the mBJ-GGA approximation that is yielding the more accurate values. We investigated the physical properties of LuNiZ (Z = Bi, Sb) with a valence electrons number of 18. The main conclusions can be summarized as follows: The compounds of LuNiBi and LuNiSb have small indirect gaps following the Γ-X direction, where the valence band maximum is located at point Γ and the conduction band minimum is at point X. Consequently, both materials present a semiconductor character. The valence band of each compound is mainly dominated by the states of the Lu-f and Ni-d orbitals, with small contribution from the Bi-s, Bi-p, Sb-s, and Sb-p orbitals for LuNiBi and LuNiSb, respectively. However, the conduction band is characterized by hybridization of the Lu-d, Ni-d, Bi-p, and Sb-p states of LuNiBi and LuNiSb, respectively. The indirect optical gaps which are equal to LuNiBi: $E_g = 0.12$ eV and LuNiSb: $E_g = 0.22$ eV are reasonably close to other calculations. The variation of the thermal conductivity, power factor, figure of merit ZT, Seebeck coefficient, and electrical conductivity as a function of temperature have been obtained using mBJ-GGA approximation that is yielding good results for LuNiBi and LuNiSb materials which could be suitable candidates for applications in the photovoltaic and thermoelectric field. This comparative and detailed study may encourage further experimental efforts for half-Heusler thermoelectric materials in order to find materials with high thermoelectric performance and may contribute to the development of more efficient devices used in the optoelectronic and thermoelectric field.

References

1. Blaha, P., et al.: WIEN2k: an augmented plane wave plus local orbitals program for calculating crystal properties, Inst. Vienna Univ. of Technology, Physical and Theoretical Chemistry (2001)
2. Larson, P., et al.: Electronic structure of rare-earth nickel pnictides: narrow-gap thermoelectric materials. Phys. Rev. B **59**, 15660 (1999)
3. Casper, F.: Structure and properties of intermetallic ternary rare earth compounds. (2008)
4. Karla, I., Pierre, J., Ouladdiaf, B.: Magnetic structures of RNiSb compounds (R= rare earths) investigated by neutron diffraction. Phys. B **253**, 215–221 (1998)
5. Haase, M.G., et al.: Equiatomic rare earth (Ln) transition metal antimonides LnTSb (T = Rh, Ir) and bismuthides LnTBi (T = Rh, Ni, Pd, Pt). J. Solid State Chem. **168**, 18–27 (2002)
6. Chen, J., et al.: Structural and magnetotransport properties of topological trivial LuNiBi single crystals. J. Alloy. Compd. **784**, 822–826 (2019)
7. Synoradzki, K., Ciesielski, K., Kępiński, L., Kaczorowski, D.: Effect of secondary lunisn phase on thermoelectric properties of Half-Heusler alloy Lunisb. Materials Today: Proceedings **8**, 567–572 (2019)
8. Hohenberg, P., Kohn, W.: Inhomogeneous electron gas. Physical review **136**, B864 (1964)
9. Perdew, J.P., et al.: Atoms, molecules, solids, and surfaces: applications of the generalized gradient approximation for exchange and correlation. Phys. Rev. B **46**, 6671 (1992)
10. Wu, Z., Cohen, R.E.: More accurate generalized gradient approximation for solids. Physical Review B. **73**, 235116 (2006)
11. Perdew, J.P., Burke, K., Ernzerhof, M.: Generalized gradient approximation made simple. Phys. Rev. Lett. **77**, 3865 (1996)
12. Murnaghan, F.: The compressibility of media under extreme pressures. Proc. Natl. Acad. Sci. U.S.A. **30**, 244 (1944)
13. Casper, F., Felser, C.: Magnetic and electronic properties of Renibi (Re = Pr, Sm, Gd–Tm, Lu) compounds. Z. Anorg. Allg. Chem. **634**, 2418–2422 (2008)
14. Narimani, M., Nourbakhsh, Z.: Topological phase and optical properties of Lunibi bulk and nano-layer. Thin Solid Films **634**, 112–120 (2017)
15. Winiarski, M.J., Bilińska, K.: High Thermoelectric power factors of P-type Half-Heusler alloys Ynisb, Lunisb, Ypdsb, and Lupdsb. Intermetallics **108**, 55–60 (2019)
16. WINIARSKIA, M., Bilinska, K.: Power Factors of P-Type Half-Heusler alloys Scnibi, Ynibi, and Lunibi by ab initio calculations. Acta Physica Polonica, A. , 138 (2020)
17. Saini, S.M.: Structural, electronic and thermoelectric performance of narrow gap Lunisb Half Heusler compound: potential thermoelectric material. Physica B: Condensed Matter. **610**, 412823 (2021)

18. Touia, A., Ameri, M., Ameri, I.: Synthesis, crystal structure and physical properties of the thulium filled skutterudite TmFe4P12 under the effect of the pressure: LDA and LSDA calculation. Optik **126**, 3253–3259 (2015)

19. Cui, S., et al.: High-pressure structural, electronic and optical properties of KMgF3: a first-principles study. J. Alloy. Compd. **484**, 597–600 (2009)

20. Ambrosch-Draxl, C., Sofo, J.O.: Linear optical properties of solids within the full-potential linearized augmented planewave method. Comput. Phys. Commun. **175**, 1–14 (2006)

21. Aydin, S., et al.: Effect of pressure on structural, electronic, mechanical and optical properties of ruthenium diboride with oP 12-type structure. Indian J. Phys. **90**, 767–779 (2016)

22. Kramers, H.: Atti Congr. Intern. Fisico como, (1927)

23. Kronig, R.d.L.: On the theory of dispersion of x-rays. Josa. **12**, 547–557 (1926)

24. Ciftci, Y.O., Evecen, M.: First principle study of structural, electronic, mechanical, dynamic and optical properties of half-Heusler compound LiScSi under pressure. Phase Transitions **91**, 1206–1222 (2018)

25. Wei, J., Wang, G.: Thermoelectric and optical properties of half-Heusler compound TaCoSn: a first-principle study. J. Alloy. Compd. **757**, 118–123 (2018)

26. Kaur, K., Kumar, R.: Giant thermoelectric performance of novel TaIrSn Half Heusler compound. Phys. Lett. A **381**, 3760–3765 (2017)

27. Yusufu, A., et al.: Thermoelectric properties of Ag1− x GaTe2 with chalcopyrite structure. Applied Physics Letters. **99**, 061902 (2011)